Int. J. Electrochem. Sci., 11 **(2016)** 9941 – 9948, doi: 10.20964/2016.12.23

International Journal of
ELECTROCHEMICAL
SCIENCE
www.electrochemsci.org

Electrochemical Performance study of Metal ions co-doping in B-site of LTO Anode Material

Li-ge Wang[*], *Fuyun Li, Min Zeng*

School of Materials Science and Engineering, Southwest University of Science and Technology,
Mianyang 621010, P R China
E-mail: wanglige@swust.edu.cn

Received: 22 August 2016 / *Accepted:* 2 October 2016 / *Published:* 10 November 2016

Metal ions co-doped $Li_4Sb_xCr_xTi_{5-2x}O_{12}$ ($0 \leq x \leq 0.1$) anode material had been successfully synthesized by solid state reaction method. The electrochemical properties of these spinel anode materials had been investigated. The results showed that $Li_4Sb_xCr_xTi_{5-2x}O_{12}$ materials with good crystallization and the metal ions Sb^{5+}/Cr^{3+} had entered the Ti^{4+} B-site lattice without destroying or changing the crystal structure of $Li_4Ti_5O_{12}$. Compared with pristine $Li_4Ti_5O_{12}$ anode material, the $Li_4Sb_{0.05}Cr_{0.05}Ti_{4.9}O_{12}$ materials presented the best charge/discharge capacity, better reversibility and higher cyclic stability, especially at high current rates, for lithium-ion batteries.

Keywords: Metal ions co-doping, $Li_4Sb_xCr_xTi_{5-2x}O_{12}$, Anode material, lithium storage capacity

1. INTRODUCTION

As the main power source, due to their excellent performance such as high energy density, little self-discharge, no memory effect, long cycle life and environmental benignity, lithium-ion batteries (LIBs) have received tremendous attention and have been widely employed for the portable electronic devices, the electric vehicles (EVs) [1-2] and the hybrid electric vehicles (HEVs) [3-4]. This promise has motivated numerous research efforts by groups, seeking to develop both high capacity and good cyclic stability materials. Compared with the carbon-based anode materials that had been commercial applied, spinel $Li_4Ti_5O_{12}$ (LTO) has been regarded as a most promising electrode material of LIBs, since it has excellent Li ions insertion/extraction cyclic reversibility, higher theoretical capacity (175 $mAhg^{-1}$) and almost zero volume change during charge/discharge process [1-4]. Unfortunately, due to the pretty low electronic conductivity of pure LTO material, its rate performance is limited and the electrochemical performance is also poor [5].

Several effective ways have been proposed to improve the conductivities, including synthesis of nano-materials [6,7], doping with metal or nonmetal ions (such as V^{5+}, Mn^{4+}, Cr^{3+}, Mg^{2+}, N^{3-} and F^{-}) in Li^{+} (A-), Ti^{4+} (B-) or O^{2-} (C-) sites [1-2, 8-10], surface coating (such as Ag, Zn, TiN, TiO_2, SnO_2, carbon, carbon nano-tubes, or graphene) [11-16]. It was found that the substitution of B-site by Metal ions can increase the amount of mixing Ti^{3+} and Ti^{4+} and increase the electronic conductivity, because of the charge compensation [17-18]. In this paper, Metal co-doped LTO powders were prepared by solid state reaction method and the effect of Sb^{5+}/Cr^{3+} co-doping on the physical and electrochemical performance of $Li_4Sb_xCr_xTi_{5-2x}O_{12}$ was systematically investigated. The average valence state of Sb^{5+} and Cr^{3+} is equal to that of Ti^{4+}, and the ionic radius of Sb^{5+} (0.60 Å) and Cr^{3+} (0.615 Å) are also comparable to that of Ti^{4+} (0.605 Å) [1]. Therefore, it is considered that the B-site substitution by Sb^{5+} and Cr^{3+} ions is possible, which should lead to increase the electron concentration and conductivity.

2. EXPERIMENTAL PROCEDURE

2.1. Preparation of metal ions co-doped $Li_4Ti_5O_{12}$

The pristine $Li_4Ti_5O_{12}$ and metal ions co-doped $Li_4Sb_xCr_xTi_{5-2x}O_{12}$ samples were synthesized by the traditional solid state reaction method [8]. The raw materials consisted of TiO_2 (P25 Nano-material, Hetachroma), Li_2CO_3 (AR, Chengdu Kelong Chemical Agents Co. Ltd), Sb_2O_5 (AR, Chengdu Chemical Agents Co. Ltd) and Cr_2O_3 (AR, Chengdu Chemical Agents Co. Ltd) according to the stoichiometric quantities of $Li_4Sb_xCr_xTi_{5-2x}O_{12}$ (x=0~0.1). The required molar ratios raw materials were mixed, ball milled with ethanol, and then sintered at 800°C for 12 h to prepare the Sb-Cr-LTO. During the sintering process, slightly excess Li_2CO_3 was added to compensate for Li volatilization [9].

2.2. Materials characterizations and testing

The synthetic samples were measured by XRD (X-ray diffraction) using an X'Pert PRO (PANalytical) with a Cu-K_α radiation. The morphologies of the samples were characterised on TEM (transmission electron microscope), HRTEM (high-resolution TEM) and SAED (selected area electron diffraction, Tecnai F20, FEI). The working electrodes were fabricated by mixing 80 wt% active anode materials with 10 wt% conductive carbon black and 10 wt% PVDF (polyvinylidene difluoride), and then wet mixed in an agate mortar, with an appropriate amount of NMP (N-methyl-pyrrolidone) solvent to form homogeneous slurry. The slurry was coated on a Cu foil and vacuum dried overnight at 120°C to remove the solvent. The electrochemical tests were investigated using CR2016-type coin cells, with pure Li foil as the counter electrode, the polypropylene micro-porous films (Celgard 2300) as the separators, and 1 M $LiPF_6$ dissolved in a volume ratio 1:1:1 of EC (ethylene carbonate), DEC (diethyl carbonate), and DMC (dimethyl carbonate) as the electrolyte. The coin cells were assembled in an Ar-filled glove box and standing for 12h before testing. The galvanostatic charge/discharge measurements at room temperature were performed on a LAND test system at constant current densities 1 C, within the voltage range of 1.0-2.5 V (vs. Li/Li+). The charge rate performance also had been measured at different current densities from 1C to 10C. Electrochemical impedance spectroscopy (EIS) was conducted on a CHI760C electrochemical station from 0.01 Hz to 100 kHz. All the specific capacities were calculated based on the overall mass of the LTO and Sb-Cr-LTO.

3. RESULTS AND DISCUSSION

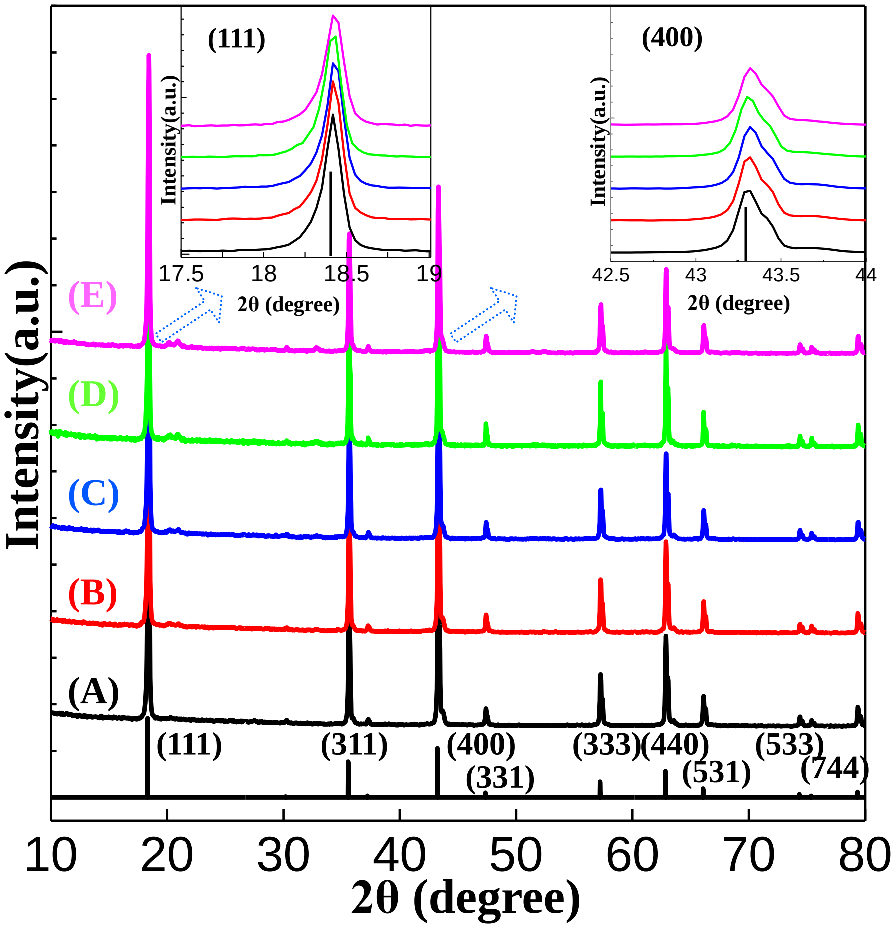

Figure 1. XRD patterns of the $Li_4Sb_xCr_xTi_{5-2x}O_{12}$ powders: (A) X=0, (B) X=0.025, (C) X=0.05, (D) X=0.075, (E) X=0.1, respectively.

As shown in Fig.1, the XRD patterns of the $Li_4Sb_xCr_xTi_{5-2x}O_{12}$ ($0 \leq x \leq 0.1$) samples display well-defined diffraction peaks within the 2θ range from 10° to 80°. The XRD patterns of Sb-Cr-LTO samples agreed well with the spinel phase $Li_4Ti_5O_{12}$ (JCPDS No.49-0207, Fd-3m, a=b=c=8.359Å) [1]. The diffraction peaks of the samples were sharp and strong, suggesting their high crystallinity. No impure-phases related peaks were detected in the XRD patterns of $Li_4Sb_xCr_xTi_{5-2x}O_{12}$ ($x \leq 0.075$), showing that the metal ions Sb^{5+}/Cr^{3+} had entered the $Li_4Ti_5O_{12}$ crystal lattice and co-replaced for Ti^{4+}-site, without forming a new phase or changing the crystal structure of pristine $Li_4Ti_5O_{12}$. However, for x>0.075, a few impurity peaks had been observed in the XRD patterns, which also shown that there is a limit to the co-doping amount for $Li_4Ti_5O_{12}$. As shown in the insert of Fig. 1, since the ionic radius of

Sb^{5+} and Cr^{3+} are also comparable to that of Ti^{4+}, the (111) and (400) peak position angle almost unchanged with the Metal ion content increasing [1]. The mean crystal sizes of the samples calculated from the Scherrer equation are about 70 nm, 85 nm, 78 nm, 89 nm and 96 nm, respectively.

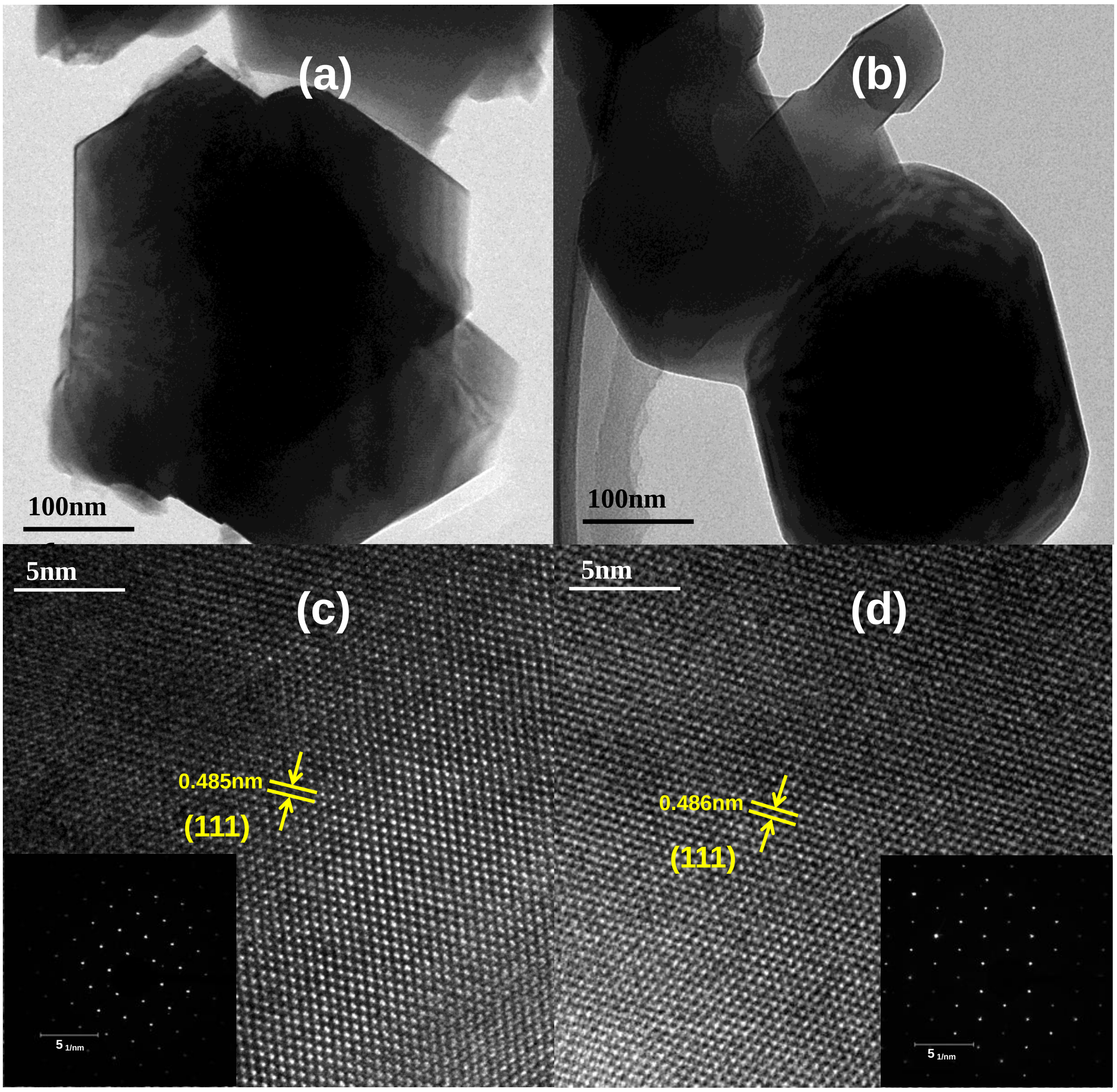

Figure 2. The TEM image, HRTEM image and SAED diagram of the sample: (a) (c) pure $Li_4Ti_5O_{12}$, (b) (d) $Li_4Sb_{0.05}Cr_{0.05}Ti_{4.9}O_{12}$, respectively.

The typical TEM images of the pristine $Li_4Ti_5O_{12}$ and the $Li_4Sb_xCr_xTi_{5-2x}O_{12}$ (X=0.05) sample were shown in Fig. 2(a) and 2(b). From the TEM images, we can observe that the samples are composed of irregular particles around 200 nm. Compared with the pristine LTO, Sb-Cr-LTO sample had smaller grain size, indicating that metal ions doping can effectively inhibit the crystal growth. On the other hand, smaller size is also conducive to enhance the electrochemical performance, because it will make the electrode material contact with electrolyte more adequately. As can be seen from

HRTEM, the interplanar spacing is ca. 4.85 Å (in Fig. 2(c)), corresponding to (111) lattice plane of LTO. However, the interplanar spacing (111) of the doped material is ca. 4.86 Å (in Fig. 2(d)), which is a bit bigger than the undoped one. The changing trend of the lattice parameters is related to the metal ions radius and doping amount. Since the mean ionic radius of Sb^{5+} and Cr^{3+} is slightly bigger than that of Ti^{4+}, the interplanar spacing increased with the increasing of doping amount. This suggests that Sb^{5+}/Cr^{3+} ions had entered the Ti-sites of the LTO crystal lattice and did not produced adverse structure distortion [9]. The insets in Fig. 2(c) and 2(d) indicate the selected area electron diffraction pattern of the samples. The regular distribution of sharp spots reveals that the materials are monocrystal and has a good crystal structure.

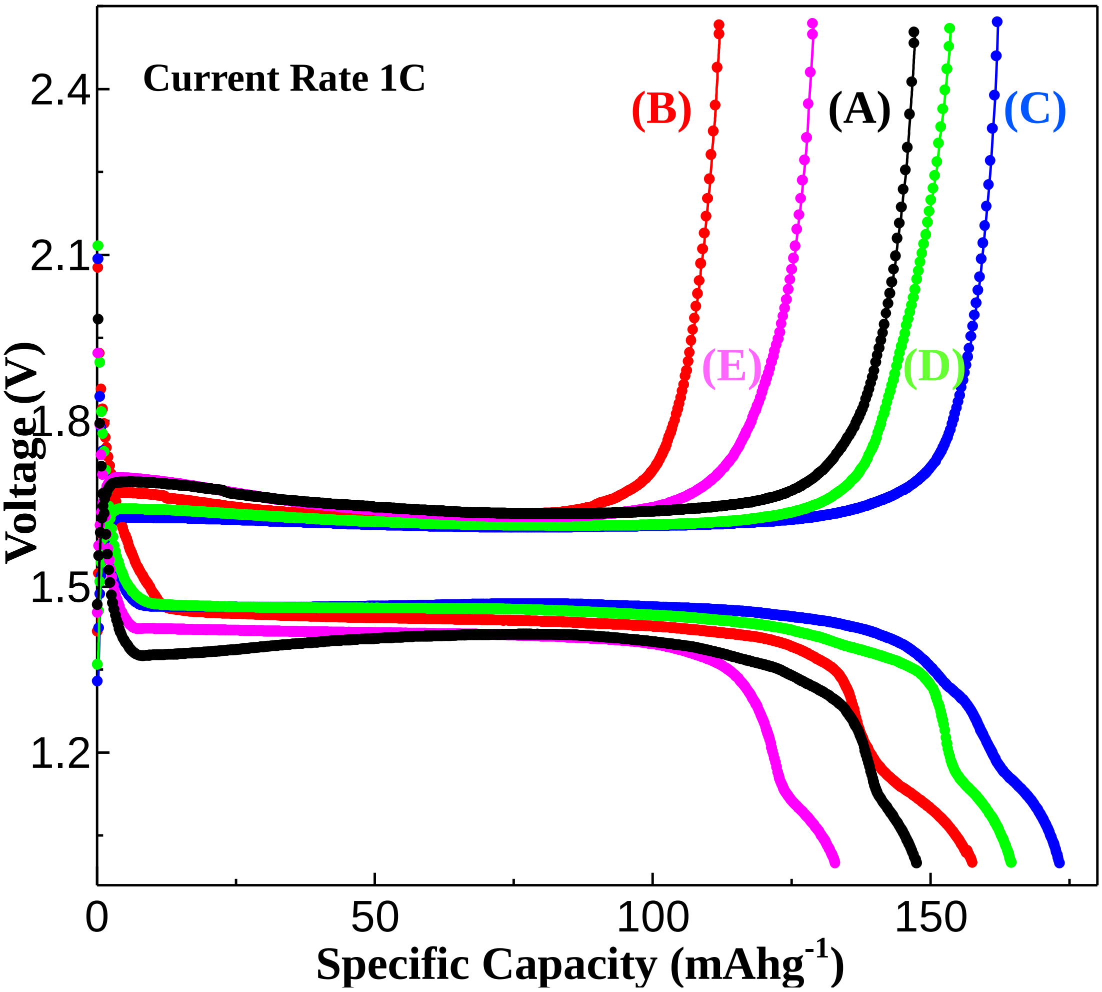

Figure 3. Initial charge/discharge curves with current rate 1C of the as-prepared $Li_4Sb_xCr_xTi_{5-2x}O_{12}$ cells: (A) X=0, (B) X=0.025, (C) X=0.05, (D) X=0.075, and (E) X=0.1, respectively

The initial charge and discharge galvanostatic curves of all samples at 1 C are shown in Fig. 3. It can be seen that the $Li_4Sb_xCr_xTi_{5-2x}O_{12}$ samples displayed the first discharge capacities of 153.1 (X=0, A), 107.8 (X=0.025, B), 166.7 (X=0.05, C), 156.3 (X=0.075, D), and 140.55 (X=0.1, E) mAhg^{-1}, respectively, which very close to the theoretical capacity of LTO as shown in the other literature

[1,8,9]. From the charge/discharge curves of the samples, the flat plateau position at about 1.7 V and 1.5 V can be found, and it can be attributed to the oxidation-reduction reactions of Ti^{4+}/Ti^{3+} in $Li_4Ti_5O_{12}$ [1]. With the increase of doping ions, the charging voltage reduced and the discharge voltage rose. This suggests that the co-doping of Sb^{5+} and Cr^{3+} ions reduced the polarization in the charge/discharge process. In addition, it can be noted that a small discharge plateau is observed at about 1.1 V. These peaks can be ascribed to the phase transformation of impurity. However, there is no any signal in the charging process, this may be due to the charging platform of impurity is higher than 2.5 V (vs. Li/Li^{+}) [1].

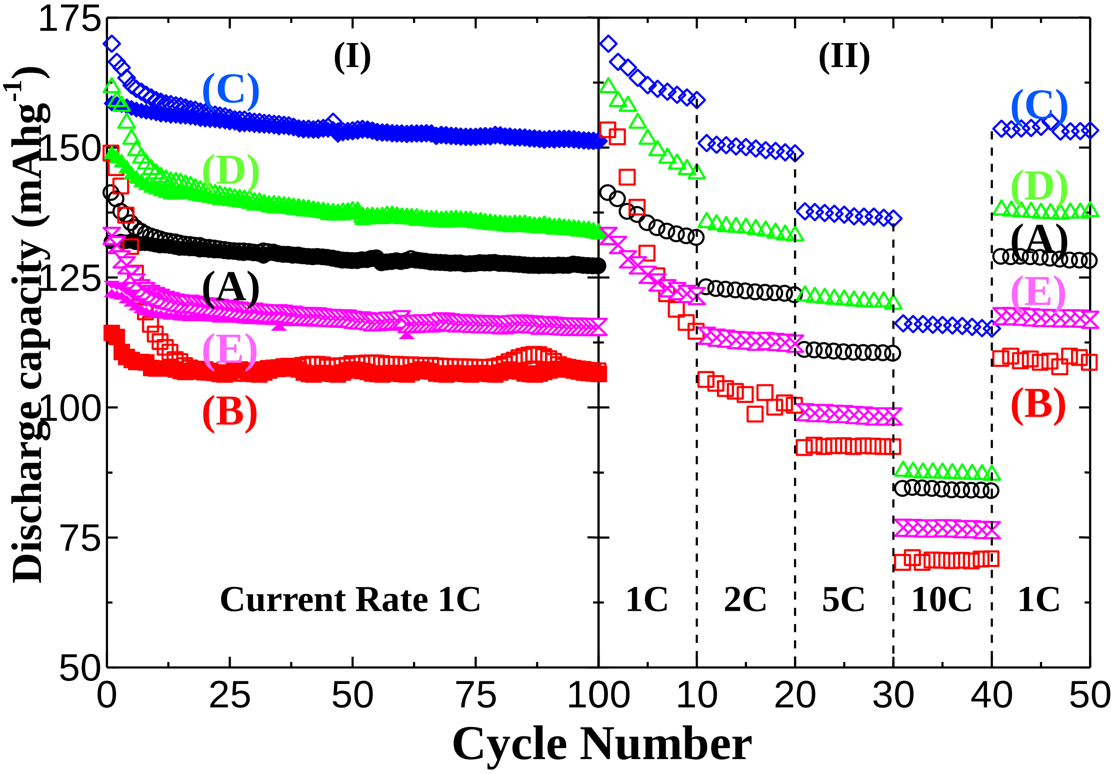

Figure 4. The electrochemical properties of (I) cycling performance at a rate of 1C and (II) specific capacities at different C rates, of the pure $Li_4Ti_5O_{12}$ powders and doped powders $Li_4Ti_{5-2x}Cr_xSb_xO_{12}$: (A) X=0, (B) X=0.025, (C) X=0.05, (D) X=0.075, (E) X=0.1, respectively.

Fig. 4(I) shows the long-term cycling performance of the as-prepared samples with a constant current density of 1C between 1.0 V and 2.5 V for 100 cycles. Among these Sb^{5+}/Cr^{3+} co-doped samples, only the capacity and cycle performance of the $Li_4Sb_xCr_xTi_{5-2x}O_{12}$ (x=0.05 and 0.075) sample is larger than the pristine $Li_4Ti_5O_{12}$, although all of the electrodes show good cycling stability at 1C. This may be due to the synergistic effect of doping and compositing [1]. The rate performance of the doped material, as shown in Fig. 4(II), was also investigated through varying the charge-discharge rate. The $Li_4Sb_{0.05}Cr_{0.05}Ti_{4.9}O_{12}$ sample displayed the discharge capacities of 167, 155, 138 and 115 mAhg^{-1}, which is higher than that of pristine LTO 140, 123, 110 and 83 mAhg^{-1}, at rates of 1, 2, 5 and 10 C, respectively. The above discussions indicate that Sb^{5+}/Cr^{3+} co-doped material has practical applications in rapid charge/discharge energy storage systems.

Electrochemical impedance spectroscopy (EIS) was carried out to understand the mechanism of improved performance of Sb^{5+}/Cr^{3+} co-doped. As shown in Fig. 5, EIS curve of $Li_4Ti_5O_{12}$ and $Li_4Sb_{0.05}Cr_{0.05}Ti_{4.9}O_{12}$ electrodes was performed at room temperature, and typical Nyquist plots were fitted by a modified Randles–Ershler equivalent circuit [8, 18]. As is well known, the electrolyte resistance (Rs), which is made up of the ohmic resistance of the electrode and the solution resistance, could be obtained from the intersection of the real axis and the curve. The charge-transfer resistance (Rct), which is occured at the particle/electrolyte interface, could be calculated from the semicircle in the medium-frequency region. The Warburg impedance (Z_w) could be obtained from the inclined line in the low-frequency range [18]. In this study, the values of R_s, R_{ct} and Z_w of $Li_4Sb_{0.05}Cr_{0.05}Ti_{4.9}O_{12}$ are smaller than that of $Li_4Ti_5O_{12}$ from the EIS simulated data by the equivalent circuit. The diffusion coefficient of Li^+ ion was calculated to be 3.3×10^{-13} $cm^2\cdot s^{-1}$ for $Li_4Ti_5O_{12}$ and 1.3×10^{-12} $cm^2\cdot s^{-1}$ for $Li_4Sb_{0.05}Cr_{0.05}Ti_{4.9}O_{12}$, from the formula as shown in literature [19]. Therefore, this result demonstrated that Sb^{5+}/Cr^{3+} co-doping can effectively restrain the charge-transfer resistance of LTO electrodes and enhanced the Li^+ diffusion, which directly affects the battery performance.

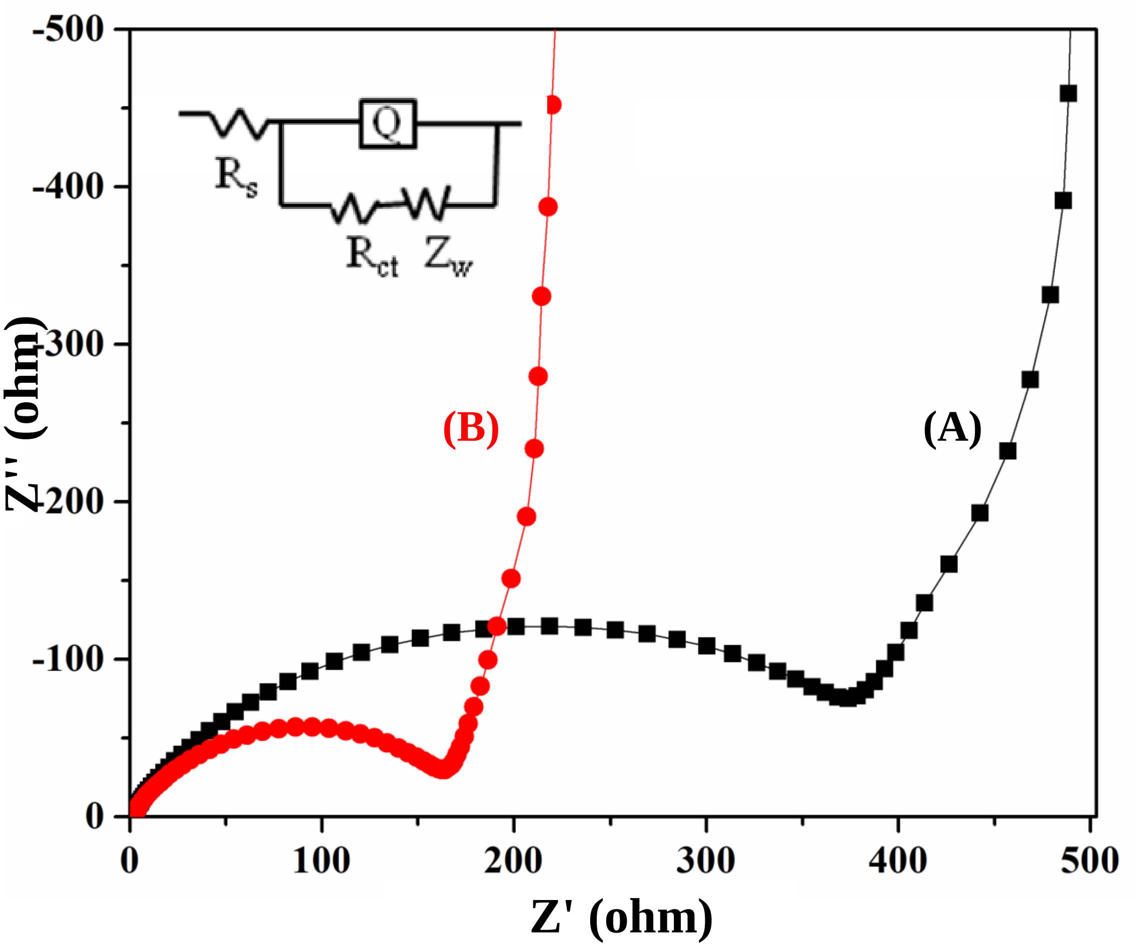

Figure 5. The EIS curve and Nyquist plots of (A) $Li_4Ti_5O_{12}$ and (B) $Li_4Sb_{0.05}Cr_{0.05}Ti_{4.9}O_{12}$ at room temperature.

4. CONCLUSIONS

By solid-state reaction method, Metal ion co-doped LTO powders have been successfully synthesized. XRD patterns show that all Metal ion co-doped materials have good crystallinity and high phase purity. With increasing of the co-doping amount, the lattice parameter is observed almost unchanged. From the above discussion, it can be seen that the Sb^{5+}/Cr^{3+} ions had entered the lattice B-site of $Li_4Ti_5O_{12}$ without destroying the crystal structure of pristine $Li_4Ti_5O_{12}$ or forming a new phase. The $Li_4Sb_{0.05}Cr_{0.05}Ti_{4.9}O_{12}$ electrode presents a higher specific capacity and better cycling performance than the LTO electrode prepared by the similar process. $Li_4Sb_{0.05}Cr_{0.05}Ti_{4.9}O_{12}$ exhibits a specific capacity of 167mAhg^{-1} at 1C. All the evidences demonstrate that the $Li_4Sb_{0.05}Cr_{0.05}Ti_{4.9}O_{12}$ electrode is a promising anode material for Li-ion batteries.

References

1. H. Song, S.W. Yun, H.H. Chun, M.G. Kim, K.Y. Chung, H.S. Kim, B.W. Cho, Y.T. Kim, *Energy Environ. Sci.*, 5 (2012) 9903
2. D. Li, Y. Sun, X. Liu, R. Peng, H. Zhou, *Chem. Sci.*, 6 (2015) 4066.
3. Y. C. Kuo, J. Y. Lin, *Electrochimi. Acta.*, 142 (2014) 43.
4. S. Chen, Y. L. Xin, Y. Y. Zhou, L. M. Qi, *Environ. Sci.*, 7 (2014) 1924.
5. C. H. Chen, J. T. Vaughey, A. N. Jansen, M. M. Thackeray, *J. Electrochem. Soc.*, 148 (2001) 102.
6. W. Wang, B. Jiang, S. Q. Jiao, *Electrochimi. Acta.*, 114 (2013) 198.
7. L. F. Shen, X. G. Zhang, E. Uchaker, G. Z. Cao, Adv. *Energy. Mater.*, 2 (2012) 691
8. F. Y. Li, M. Zeng, J. Li, H. Xu, *Int. J. Electrochem. Sci.*, 10 (2015) 10445.
9. M. D. Ji, Y. L. Xu, Z. Zhao, H. Zhang, *J. Power. Sources.*, 263 (2014) 296.
10. H. D. Yoo, Y. L. Liang, Y. Yao, *ACS. Appl. Mater. Interfaces.*, 7 (2015) 7001.
11. S.H. Huang, Z.Y. Wen, B. Lin, J.D. Han, X.G. Xu, *J. Alloy. Compd.*, 457 (2008) 400.
12. Y. Q. Wang, L. Gu, Y. G. Guo, H. Li, X.Q. He, S. Tsukimoto, Y. Ikuhara, L.J. Wan, *J. Am. Chem. Soc.*, 134 (2012) 7874.
13. Y. Wang, A. J. Zhou, X. Y. Dai, L.D. Feng, J.W. Li , J.Z. Li, *J. Power Sources*, 266 (2014) 114.
14. H. Q. Zhang, Q. J. Deng, C. X. Mou, Z.L. Huang, Y. Wang, A.J. Zhou, J.Z. Li, *J. Power Sources*, 239 (2013) 538.
15. L. P. Wang, H. Q. Zhang, Q.J. Deng, Z.L. Huang, A.J. Zhou, J.Z. Li, *Electrochim. Acta.*, 142 (2014) 202.
16. Y. G. Wang, H. M. Liu, K. X. Wang, H. Eiji, Y. R. Wang, H. S. Zhou, *J. Mater. Chem.*, 19 (2009) 6789.
17. T. F. Yi, B. Chen, H. Y. Shen, R.S. Zhu, A.N. Zhou, H.B. Qiao, *J. Alloy. Compd.*, 558 (2013) 11.
18. F. Y. Li, M. Zeng, J. Li, X.L. Tong, H. Xu, *RSC Adv.*, 6 (2016) 26902.
19. X. Wang, H. Hao, J. Liu, T. Huang, A.S. Yu. *Electrochim. Acta.*, 56 (2011) 4065.